

# Aberration correction in an optical lattice setup

**Student Paper**

**Author(s):**

Poitrinal, Martin

**Publication date:**

2024

**Permanent link:**

<https://doi.org/10.3929/ethz-b-000687947>

**Rights / license:**

[In Copyright - Non-Commercial Use Permitted](#)



Eidgenössische Technische Hochschule Zürich  
Swiss Federal Institute of Technology Zurich

# Aberration correction in an optical lattice setup

Semester Thesis

Martin Poitrinal  
mpoitrinal@ethz.ch

Quantum Optics Laboratory  
Departement of Physics, D-PHYS  
ETH Zürich

**Supervisors:**  
Samuel Jele  
Marius Gächter  
Dr. Konrad Viebahn

July 23, 2024

I would like to warmly thank Samuel Jele for his patience and advises. This was my first ever experimental project and I could not have hoped for a better supervisor.

# Abstract

The Quantum Optics laboratory is pioneering a unique "accordion lattice" in its new experiment. Unlike already existing lattice experiments that implement an accordion lattice using mechanically actuated mirrors, here acousto-optic deflectors will be used, eliminating mechanical vibrations. It has already been shown that the optical aberrations from off-the-shelf lenses for projecting the accordion lattice are not tolerable.

To address the challenge, we developed a workflow incorporating a Shack-Hartmann wavefront sensor to characterize aberrations of optical components and the software Zemax Optics Studio to optimize the positioning of these components. Furthermore, mechanical precision mounts were designed for the objective. After the assembly, the wavefront sensor can be used to verify the performance of the designed optical system. The measurement of the aberrations of components comprising the optical system using the wavefront sensor did not agree with the values supplied by Zemax for off-the-shelf lenses. We attribute this discrepancy to the high sensitivity to misalignment of the measurement setup, masking the intrinsic aberrations. Therefore, a more refined measurement technique has to be developed in order to measure aberrations more precisely.

# Contents

<b>Acknowledgements</b>	<b>ii</b>
<b>Abstract</b>	<b>iii</b>
<b>1 Aberration in an optical lattice setup</b>	<b>1</b>
1.1 The new accordion lattice setup . . . . .	1
1.2 Optical aberration theory and Zernike expansion . . . . .	2
1.3 Relating Ray and wave optics . . . . .	4
<b>2 Simulating and optimizing an optical setup</b>	<b>7</b>
2.1 Oslo and Zemax ray tracing softwares . . . . .	7
2.2 Zernike polynomials and setup optimization . . . . .	8
2.3 FUSION 3D design and workflow . . . . .	9
<b>3 Experimental realisation</b>	<b>11</b>
3.1 The Shack-Hartmann wavefront sensor . . . . .	11
3.2 A double pass experimental setup . . . . .	12
3.3 Experimental results and discrepancies with simulation . . . . .	14
3.4 Conclusion and outlook . . . . .	15

# Aberration in an optical lattice setup

## 1.1 The new accordion lattice setup

The new lattice experiment currently being built in the Lattice team of the Quantum Optics group relies on a new key ingredient developed in the master thesis work of Simon Wili [1]: the accordion lattice setup. By using two laser beams whose interfering angle we control via acousto optical deflectors, we can effectively control the lattice constant  $a$ .

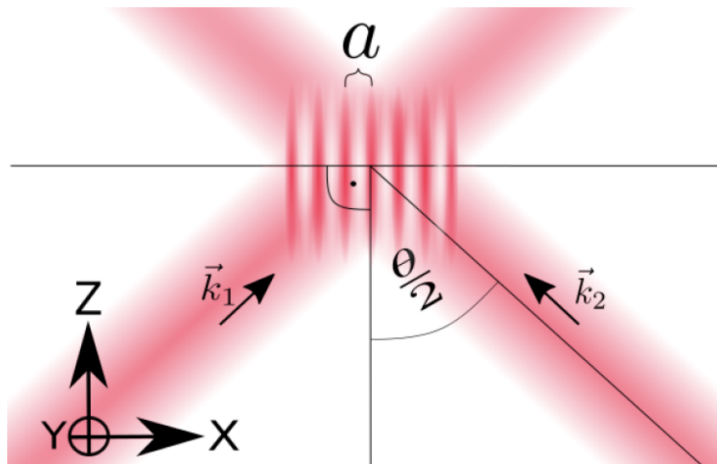


Figure 1.1: To produce an accordion lattice, two laser beams interfere at a varying angle  $\theta$  resulting in different lattice constant  $a$ . Fig Taken from Ref.[1].

This new feature introduces an additional element of concern: the two laser beams in the accordion lattice setup are focused using convex lenses that are struck at different incidence angles. In Ref.[1], this situation was modelled using an acousto-optic deflector and the resulting variation in focal length has been observed. This showed that the amount of induced variation for off the shelf lenses is not acceptable for the new setup.

In this work, we aim to expand upon these findings by developing a workflow for

## 1 Aberration in an optical lattice setup

measuring the complete aberration profile of different optical objectives, constructing custom-made optical objectives that limit targeted aberrations, and compare the simulated and measured wavefronts. Our goal is to ensure that the setup allows for only a specified amount of aberrations for a range of different incidence angles on both of the interfering beams. By following this workflow, we hope to improve the overall performance of the accordion lattice setup and reduce the impact of aberrations on this particular system. The complete description of the effect of optical aberrations on the intensity profile of the lattice is a different direction of the same project but it was not chosen due to the time constraints of a semester thesis.

Though the motivation for the thesis is the accordion lattice, we aim at developing a workflow that would be general. In this manner, any optical system could make a use of it in order to decrease optical aberrations.

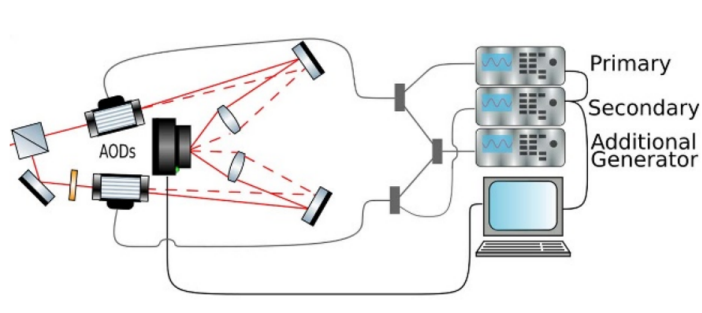


Figure 1.2: The two convex lenses are hit at varying angles using Acousto optic deflectors. Fig Taken from Ref.[1].

To better characterize optical aberrations in our system let us first describe how they are defined and can be mathematically understood with the Zernike polynomials Theory.

## 1.2 Optical aberration theory and Zernike expansion

Optical aberrations are defined in Wolf and Born's principles of optics as "deviations to the gaussian theory" [2]. They can thus be understood as additional modifications to the path of the beam that lead to non gaussian propagation terms. We can describe optical aberrations in both Ray and Wave Optics by taking as the variable of interest the deformed wavefront (Wave Optics) or the distance from the gaussian image point to the real image point (Ray Optics) [2].

The Zernike treatment of aberrations relies on an orthonormal decomposition of the wave front. The use of the Zernike polynomial basis allows to obtain mutually independent coefficients that each correspond to a specific effect in the image plain. We consider an optical field  $E(\mathbf{r}, t)$  ( $\mathbf{r}$  is the position vector) and develop its wavefront on the Zernike basis :

$$E(\mathbf{r}, t) = E_0(\mathbf{r}, t)e^{i\phi(\mathbf{r})}$$

## 1.2 Optical aberration theory and Zernike expansion

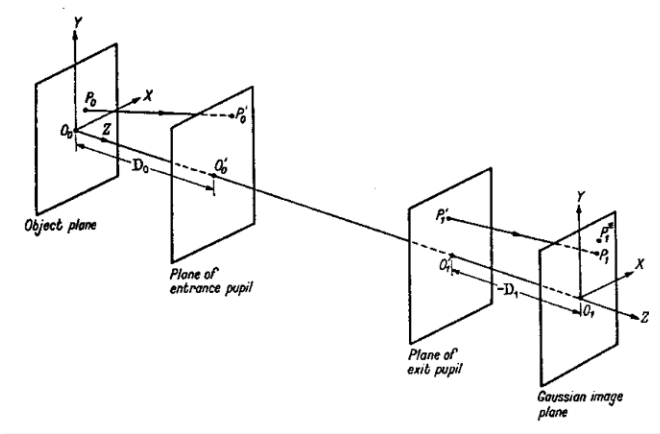


Figure 1.3: In an aberrated setup the gaussian image point is distant from the real image point. Fig taken from Ref.[2].

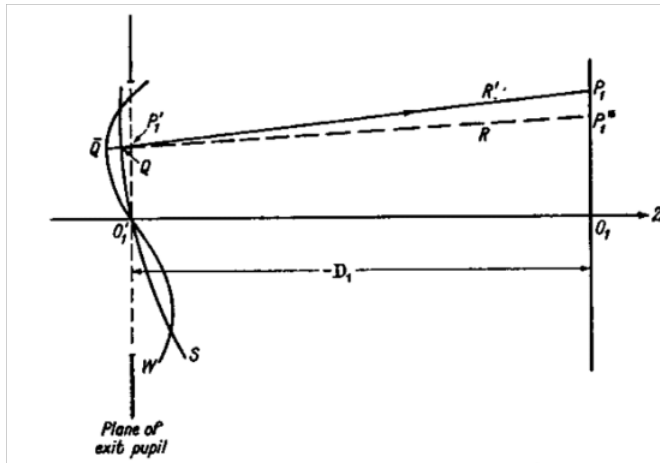


Figure 1.4: Optical aberrations can be explained in terms of ray or wave optics. The distinction resides in looking at the difference between the ideal wavefront and the real one or the ideal image point and the real one. Fig taken from Ref.[2].

We now move polar coordinates:  $\rho$  denotes the distance to the optical axis,  $\theta$  is the polar angle with respect to that same optical axis and  $z$  is the direction of propagation of the field.

$$E(\mathbf{r}, t) = E_0(\mathbf{r}, t)e^{i\phi_0(z)}e^{i\phi_1(\rho, \theta)}$$

We can decompose  $\phi_1$  into the Zernike basis  $(Z_n^m)_{(m,n) \in N^2}$  as it forms an orthonormal basis of  $R^2$ .

$$E(\mathbf{r}, t) = E_0(\mathbf{r}, t)e^{i\phi_0(z)}e^{i\sum_{m,n} a_{m,n} Z_n^m(\rho, \theta)}$$



## 1 Aberration in an optical lattice setup

The  $Z_n^m$  polynomials can further be decomposed into the product of a radial and angular part [3].

$$E(\mathbf{r}, t) = E_0(\mathbf{r}, t) e^{i\phi_0(z)} e^{i \sum_{m,n} a_{m,n} R_n^m(\rho) \cos(m\phi)}$$

To an aberrated wavefront, we can then relate a list of Zernike coefficients ( $a_{m,n}$ ). Each of the  $a_{m,n}$  coefficient describes the weight of the  $Z_{m,n}$  polynomial in the decomposition. In turn these  $Z_{m,n}$  polynomials have different effects on the image plane as can be seen on Fig.1.4 shows. Additionally, since those polynomials form an orthonormal basis, their individual effect can be taken separately from the rest. We can for instance cite the second and third Zernike polynomials, tilt X and tilt Y which displace the focal point in the X and Y direction. Their wavefronts are drawn on Fig.1.5, they correspond to a linear grating where the period is related to the amount of displacement.

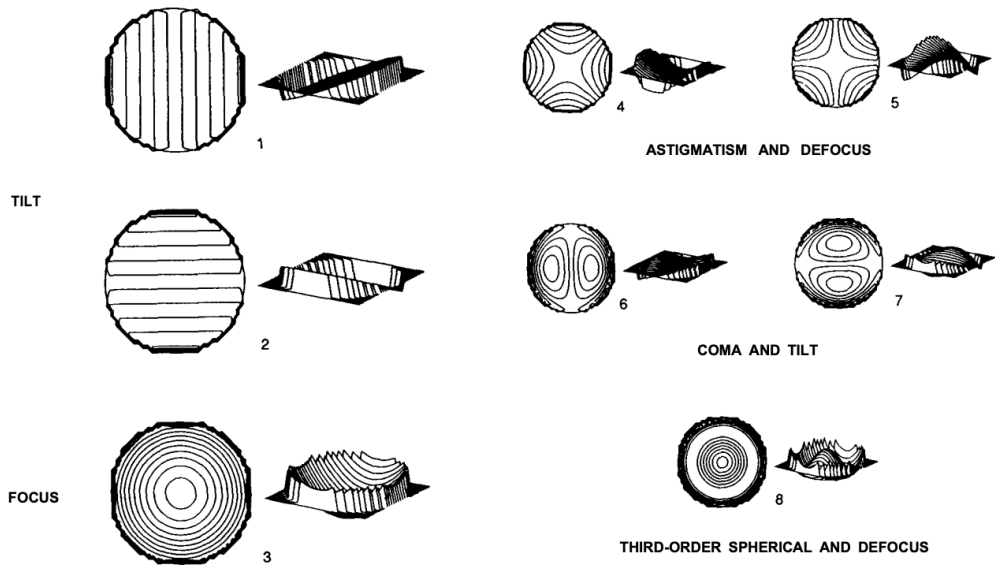


Figure 1.5: Wavefronts of the 8 first Zernike polynomials and their corresponding optical aberration. Fig taken from Ref.[4].

The ability to measure a Zernike wavefront can thus give hints on the effects of the aberrations present on the optical system on the imaging plane. This is done by relating Ray and wave optics for each coefficient to deduce its specific effect.

### 1.3 Relating Ray and wave optics

For the specific case of our system, the best description we would like is the effect on the intensity potential which is non other than the image plane. A given Zernike polynomial  $Z_{m,n}$  can be related to an effect on the image plane by calculating what the wavefront looks like.

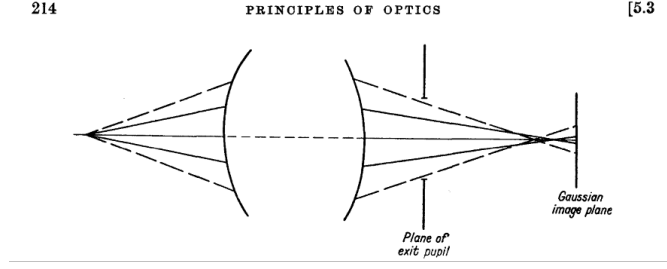


Figure 1.6: In the case of spherical aberration, rays that hit at varying angles of incidence will have a different focal length different than that of the ideal lens. Fig taken from Ref.[2].

We consider a radially symmetric TEM<sub>00</sub> gaussian beam. Similar as before,  $\rho$  is the distance to the optical axis,  $z$  is the coordinate in the direction of the optical axis.

$$\mathbf{E}(\rho, z) = E_0 \mathbf{u}_x \frac{\omega_0}{\omega(z)} \exp\left(\frac{-\rho^2}{\omega(z)}\right) \exp\left(-i\left(kz + k\frac{\rho^2}{2R(z)} - \psi(z)\right)\right)$$

If the beam is aberrated only by the  $Z_{0,2}$  ( $Z_{0,2} = a_{0,2}(\sqrt{3}(2\rho^2 - 1))$ ) defocus aberrations we obtain

$$\mathbf{E}(\rho, z) = E_0 \mathbf{u}_x \frac{\omega_0}{\omega(z)} \exp\left(\frac{-\rho^2}{\omega(z)}\right) \exp\left(-i\left(kz + k\frac{\rho^2}{2R(z)} - \psi(z)\right)\right) \exp\left(ia_{0,2}(\sqrt{3}(2\rho^2 - 1))\right)$$

$$\mathbf{E}(\rho, z) = E_0 \mathbf{u}_x \frac{\omega_0}{\omega(z)} \exp\left(\frac{-\rho^2}{\omega(z)}\right) \exp\left(-i\left(kz + k\rho^2\left(\frac{1}{2R(z)} - \sqrt{3}2a_{0,2}\right) - \psi_1(z)\right)\right)$$

This can be rewritten as

$$\mathbf{E}(\rho, z) = E_0 \mathbf{u}_x \frac{\omega_0}{\omega(z)} \exp\left(\frac{-\rho^2}{\omega(z)}\right) \exp\left(-i\left(kz + k\frac{\rho^2}{2R_0(z)} - \psi(z)\right)\right)$$

Where the radius of curvature  $R$  has been shifted by  $-\sqrt{3}2a_{0,2}$ . This effectively translates into a shift of the focusing point of the beam to a new focal point.

We now consider the  $Z_{0,4}$  primary spherical component which was the main focus of Ref.[1], we can write the following :

$$\mathbf{E}(\rho, z) = E_0 \mathbf{u}_x \frac{\omega_0}{\omega(z)} \exp\left(\frac{-\rho^2}{\omega(z)}\right) \exp\left(-i\left(kz + k\frac{\rho^2}{2R(z)} - \psi(z)\right)\right) \exp\left(ia_{0,4}(6\rho^4 - 6\rho^2 + 1)\right)$$

$$\mathbf{E}(\rho, z) = E_0 \mathbf{u}_x \frac{\omega_0}{\omega(z)} \exp\left(\frac{-\rho^2}{\omega(z)}\right) \exp\left(-i\left(kz + k\rho^2\left(\frac{1}{2R(z)} - 6a_{0,4}\rho^2 + 6a_{0,4}\right) - \psi_1(z)\right)\right)$$

## 1 Aberration in an optical lattice setup

This can be reinterpreted as a radius of curvature  $R_1(z)$  which depends on  $r$ .

$$R_1(z, \rho) = \frac{R(z)}{1 + 6a_{0,4}\rho^2 R(z) - 6a_{0,4}R(z)}$$

We note that as the value of  $r$  increases, there is a corresponding increase in the Radius of curvature. We can thus infer that rays hitting the lens at higher height will converge to a focal point closer to the lens as it can be seen on Fig.1.6. Similar derivations can be found in Ref.[2] for the coma and astigmatism aberrations. The Coma aberration effect is drawn on Fig.1.7.

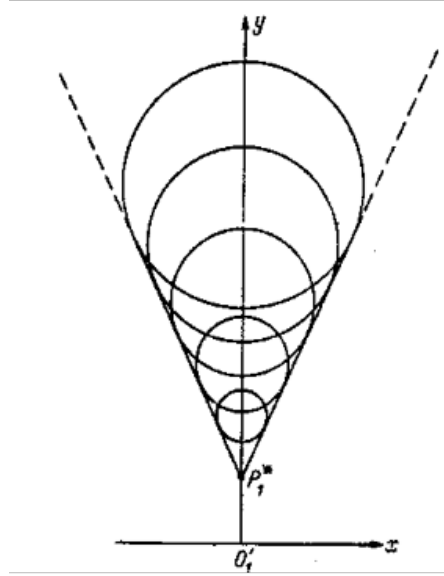


Figure 1.7: The Coma aberration effect on the focal plane involves the angular position of the intersect between ray and lens. Fig taken from Ref.[2].

This technique can be expanded by looking at the individual effects each of the Zernike polynomials on the Gaussian beam propagation. A broader and more complete description would have to include a simulation tool to encompass all aberrations and calculate their effect on the image plane by gaussian propagation methods. Ray tracing software fill this objective to get a sense of the effect of different optical aberration, they are do not simulate the full electro-magnetic field but instead trace many optical rays to deduce the behavior of the entire beam.

# Simulating and optimizing an optical setup

## 2.1 Oslo and Zemax ray tracing softwares

Oslo [5] and Zemax [6] use ray tracing to simulate a beam passing through an optical system. Their purpose in our project is to simulate the effect a given optical system has on an incoming beam and optimize it according to an objective function. Most of the simulations I did on Oslo has already been done in Ref.[1] and their was no additional result obtained.

Zemax on the other hand was used for the first time during this project and allowed for far more flexibility and different tools to work on. For instance the parameters on which Zemax allows for optimization are far more diverse than that of Oslo. We can tune the type of beam entering the setup, the thicknesses of the lenses and constitute large systems of more than 3 lenses in a much larger library than Oslo's. Additionally, Zemax can plot reconstituted wavefront, use multiple wavelengths and change the aperture of the incoming beam as well as the light source type.

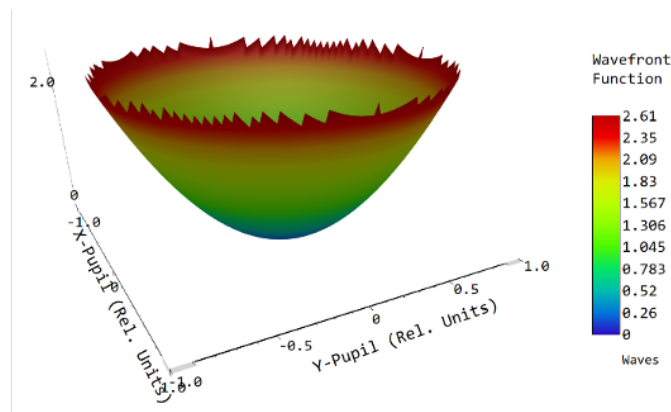


Figure 2.1: A simulated wavefront obtained by Zemax Optics Studio for a 3 lens optical system. The radial symmetry of the system is reflected on the shape of this wavefront.

## 2.2 Zernike polynomials and setup optimization

For a given experimental setup, we can visualize the different Zernike polynomials and optimize the setup for a targeted set of parameters. To do this, we input the variables we are willing to modify in the setup and specify the parameter we wish to minimize. In our case, we are targeting spherical aberration, so our parameter of interest is defined to be SPHA (the primary spherical Zernike polynomial weight). To ensure that the focal length of the combined system remains constant, we enforce this constraint by adding a penalty term to the cost function.

Before beginning the optimization process, it is important to define the type of setup we wish to build. After discussing with Marius and Samuel, we have decided to use off-the-shelf lenses and only vary the distances between them. Our approach involves combining concave and convex lenses, which have opposite contributions to spherical aberration as can be seen in Ref.[1], and optimizing the distance between them.

After running several optimizations, we find that Zemax converges to the setup drawn in Fig 2.2.

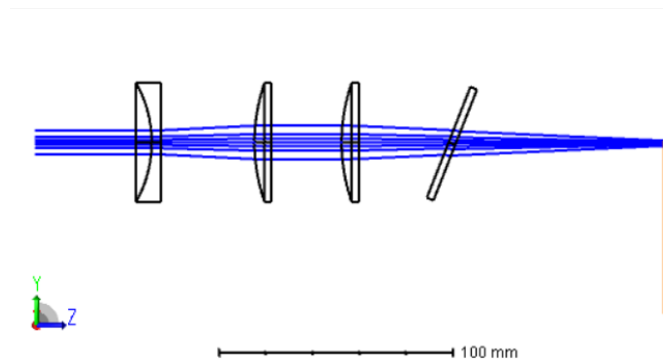


Figure 2.2: The optimized setup given by Zemax using off the shelves lenses from Thorlabs.

To get a sense of why these setups are optimal we can also plot 2D colormaps of the parameters we are studying. Plotting the SPHA contribution as a function of the distance between two of the lenses we observe Fig. 2.3 .

Running the colourmaps on the distances between convex and concave and convex and convex lenses while fixing as a constraint the focal length of the entire system shows that the configuration shown in fig 2.2 is indeed the best. This however leads us to consider how well we can create such a configuration as tilting one of the lenses a little has heavy effects on the final aberration profile. In order to ensure that these distances and orientation angles are well constrained, we designed handmade lens holders by using another Ansys software : Fusion 360 [7].

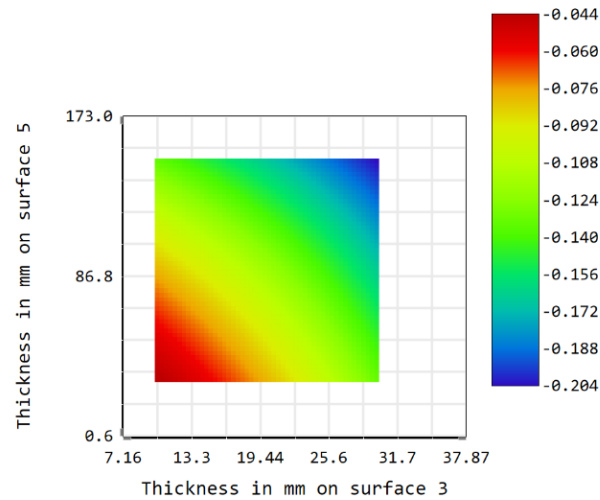


Figure 2.3: Zemax can be used to observe dependencies of various parameters by plotting 2D colour maps. Here we plot the spherical aberration coefficient SPHA as a function of two distances between lenses.

## 2.3 FUSION 3D design and workflow

If we agree with the simulations realized on Zemax, one way to build such system would be to construct "lens holders" that would need to be more precise than the Thorlabs lens 'cages'. We discussed a possible design which would consist of modular holders that allow to hold in place a lens with very low movement, each element was designed using the software Fusion 360 [7].

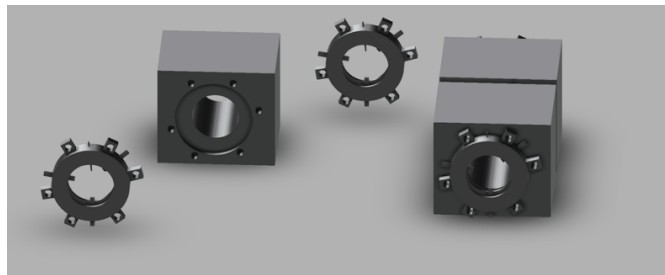


Figure 2.4: The Fusion 3D design comprises Lens Holders which are connected at fixed distances by tubes to ensure fixed distances between optical elements.

The holders are designed to be able to hold different focal lengths at high precision (less than 0.1 mm movement range allowed). Their design was discussed with the ETH engineers to maximize their stability.

With the description of the simulations, optimization and design of tailored optical

## 2 *Simulating and optimizing an optical setup*

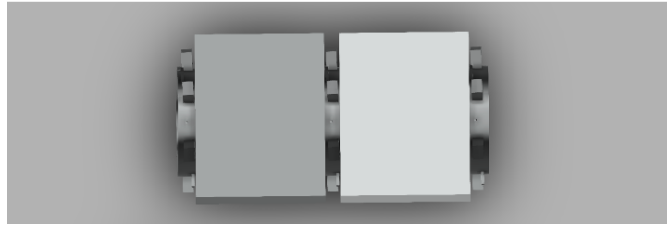


Figure 2.5: When assembled, the tubes and lens holders from a compact and robust optical system. Several tubes can be combined with the double sided holders to build more complex objectives.

objectives, we have all the elements of a potential workflow that could be used whenever there is a need of an optical system. The pattern would be the following :

- The experimental constraints determine what aberrations we care about or want to avoid.
- Zemax OpticStudio simulates an optical system comprising the elements we have in the lab, an optimization sequence is performed to obtain the best possible arrangement of the different elements for the considered objective function.
- The obtained configuration is tested accordingly using a Shack-Hartmann [3] sensor to match simulation and experiment.
- The obtained optical objective is designed using Fusion 360 and built with the ETH engineers.

# Experimental realisation

## 3.1 The Shack-Hartmann wavefront sensor

The Shack-Hartmann sensor is a powerful tool used to measure the wavefront aberrations in an optical system [3]. It operates by sampling the incoming wavefront with a lenslet array, which divides the wavefront into a series of sub-apertures. Each lenslet focuses its corresponding sub-aperture onto a detector, producing a spot pattern whose individual position relate to the local slope of the wavefront at that location. By measuring the positions of these spots relative to their ideal positions in the absence of aberrations, the Shack-Hartmann sensor can determine the local gradients of the wavefront across the entire aperture as can be seen on Fig.3.1.

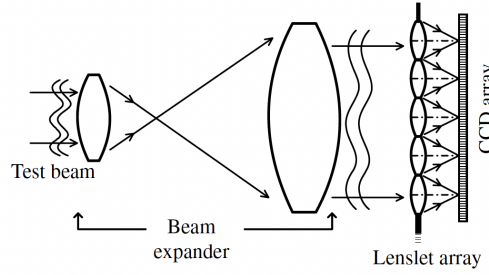


Figure 3.1: A Shack-Hartmann Camera is usually composed of a beam expander and an array of lenslets that sample the local derivatives of a wavefront. Postprocessing of the positions of the different spots on the CCD array allows to retrieve the incoming wavefront. Fig taken from Ref.[3].

$$\frac{\partial W}{\partial x_i} \approx \frac{x_i - x_{i,\text{ref}}}{f_{\text{lenslet}}}$$

$$\frac{\partial W}{\partial y_i} \approx \frac{y_i - y_{i,\text{ref}}}{f_{\text{lenslet}}}$$

We can then reconstruct the entire wavefront by integrating over these tilts :

$$W(x, y) = \int_{x,y} \frac{\partial W}{\partial y} dy + \frac{\partial W}{\partial x} dx \approx \sum_{x_i, y_i} \frac{\partial W}{\partial x_i} a_x + \frac{\partial W}{\partial y_i} a_y$$



### 3 Experimental realisation

This information is used to reconstruct the wavefront using mathematical algorithms, such as Zernike polynomial decomposition or modal reconstruction.

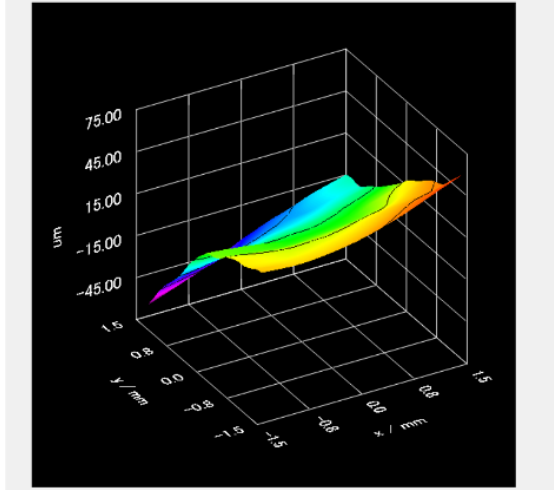


Figure 3.2: A recomposed wavefront from our Thorlabs Shack-Hartmann Camera. [8]

To ensure accurate interpolation of Zernike polynomials, it's crucial to have a sufficiently large beam for the Shack-Hartmann sensor. In our case, we aim for a beam size of a few millimeters, which aligns with the aperture of our sensor. The local derivatives measured by the Shack-Hartmann sensor are more effective at fitting a wavefront that is close to being flat. Therefore, it's beneficial to collimate the beam before it reaches the sensor, creating a wavefront reference which is flat.

Additionally, the Shack-Hartmann camera is an exceptional tool for beam collimation. The defocus aberration, which is related to the beam's curvature, is a direct indicator of collimation. A positive curvature signifies a convergent beam, while a negative curvature indicates a divergent beam. To collimate a beam, we can utilize the Shack-Hartmann sensor to measure the defocus aberration and adjust the position of the collimating lens accordingly until the Zernike coefficient for defocus is zero.

### 3.2 A double pass experimental setup

Our setup takes the form of a double pass experiment where an expander a reducer ensure that a large part of the lens is sampled so that we can effectively see the effects of the lens on the beam. Our setup is inspired from lens characterization setups [9, 10].

A quarter waveplate ensures the beam is deflected by the beam splitter after going through the optical system two times. This setup can technically accomodate any optical system as long as the focal point of the optical system matches the position of the mirror, this presupposes there is enough space between the quarter waveplate and the mirror to do so. The light comes from a 1064 nm diode laser coupled into a fiber. The model setup is drawn in Fig.3.3 and the experimental setup can be seen on Fig.3.4.

### 3.2 A double pass experimental setup

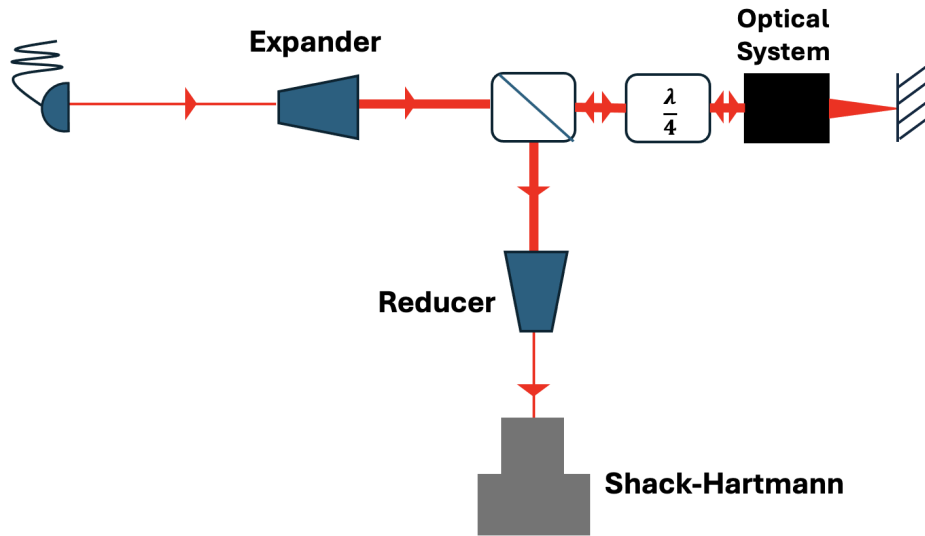


Figure 3.3: Schematic of the experimental realization of the measurement.

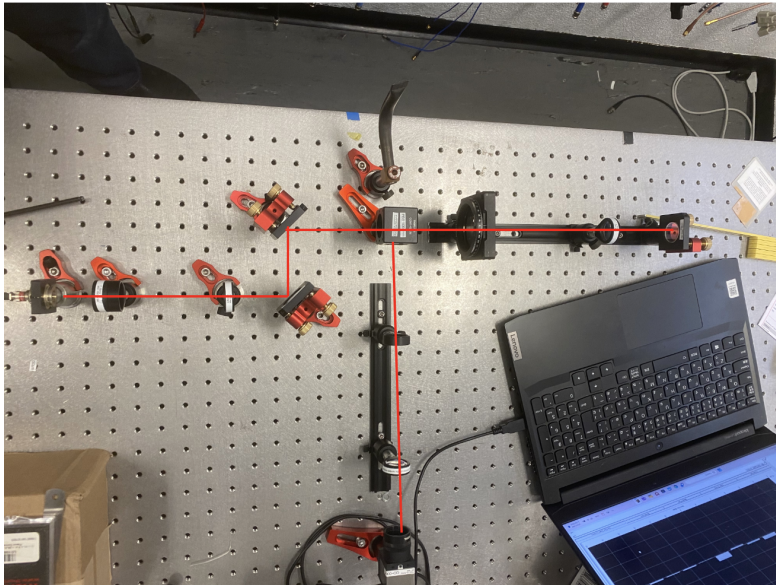


Figure 3.4: Experimental realization of the measurement, optical rails were used to ensure the alignment on the optical table plane.

Alignments proved to be crucial to obtain the right Zernike polynomials characteristics of the lens of interest. Indeed Zemax simulation showed that angular deviation of 0.01 rad already showed dominant terms that were not the one expected for a perfectly aligned

### 3 Experimental realisation

beam. Similarly for position, only a deviation of 0.1 mm can be tolerated. In order to align the beam I essentially used irises and optical rails but I retrospectively believe a more sophisticated alignment method should have been employed.

### 3.3 Experimental results and discrepancies with simulation

The simulation to which we compare our system is a 4f system where the lenses are the same as the lens of interest, this system is drawn on Fig.3.5. The Zemax Zernike analysis shows only spherical aberration when collimated as one could expect from the radial symmetry of this system.

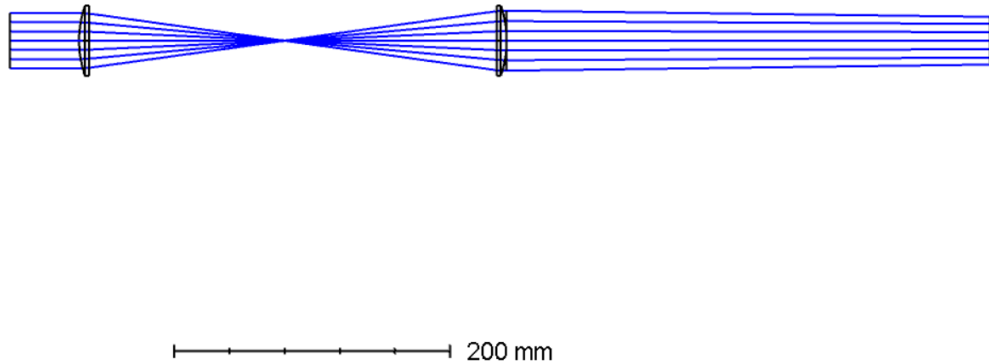


Figure 3.5: The simulation to which we compare our experimental setup is composed of two lenses forming a 4f system. This is used to simulate the behavior of the lens coupled to the mirror (at its focal point).

The measurements are done by taking the system without the lens of interest as a reference and then adding the lens of interest. The measurements of the different Zernike polynomials I obtained on the Shack-Hartmann did not match with the Zemax simulation. I observe other dominant Zernike polynomials which give a hint that misalignment may have broken the radial symmetry. One small success I could obtain is that tilting the angle in a direction gives the variation I observe on Zemax.

I identified a few sources of errors that might explain this discrepancy. First the SH sensor relies on the beam waist as the 'definition' of its fit, the larger the beam the more points are used to interpolate the coefficients. One possibility is that my beam was still too small for the SH to sample correctly the Zernike polynomials. Secondly the alignment of the lens with the incoming beam is absolutely crucial not to break the radial symmetry this as mentioned should have been done with a better alignment method. Finally I used a small focal length lens in the Reducer which was a bad idea since it means the curvature of the lens is higher and small position deviations have more effect on the wavefront. This

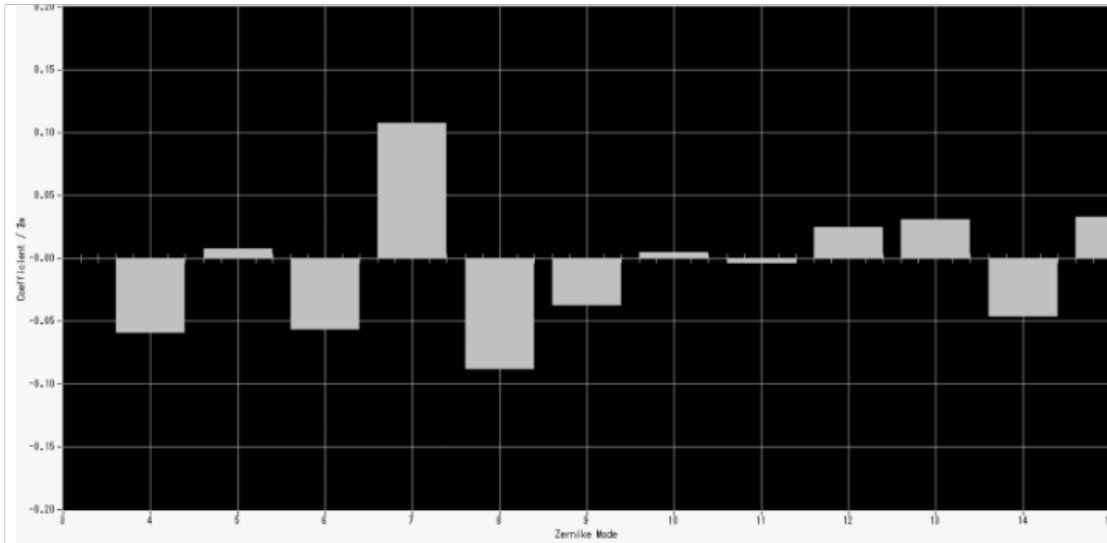


Figure 3.6: The final set of Zernike polynomials for the double pass setup obtained by the Shack Hartman sensor. The primary spherical aberration (numbered 11 here) is clearly not dominating, in contrast with the simulation.

in turns can amplify a misalignment from the lens of interest.

### 3.4 Conclusion and outlook

In this study, we developed a comprehensive workflow to design optimal optical objectives considering pre-defined constraints on optical aberrations. Using Zemax Optics Studio, we simulated an optical objective composed of off-the-shelf lenses and predicted its wavefront. The software enabled us to lower the optical aberration of the system by adjusting the distances between lenses. Once a schematic design was achieved, we used the mechanical design software Fusion 360 to create custom lens holders and tubes to maintain constant distances between lenses.

We then compared the simulated optical objective with experimental measurements using a Shack-Hartmann wavefront sensor. However, the measured values for the Zernike Polynomial expansions did not match the Zemax predictions, further investigation in Zemax suggested that misalignment in the measurement setup was the most likely cause for this discrepancy.

To effectively apply the workflow established in this study, the first step is to find a match between the simulated and measured optical objectives. Once this is accomplished, the optimal objectives should be demonstrated to outperform non-optimized ones and finally the optimized objectives can be integrated into the lattice setup using the custom optical links and holders designed with Fusion 360.

# Bibliography

1. Wili, S. *A Versatile Accordion Lattice Setup for Tweezers Experiments" in the Quantum Optics Group at ETH Zurich* MA thesis (ETH Zurich, 2021).
2. Born, M. *et al. Principles of Optics: Electromagnetic Theory of Propagation, Interference and Diffraction of Light* 7th ed. (Cambridge University Press, 1999).
3. Mansuripur, M. in *Classical Optics and its Applications* 624–631 (Cambridge University Press, 2009).
4. Wyant, J. & Creath, K. Basic Wavefront Aberration Theory for Optical Metrology. *Appl Optics Optical Eng* **11** (Jan. 1992).
5. research, L. <https://lambdares.com/oslo> Website of OSLO.
6. Ansys. <https://www.ansys.com/products/optics/ansys-zemax-opticstudio> Website of Zemax Optics Studio.
7. Autodesk. <https://www.autodesk.com/products/fusion-360/personal> Website of Fusion3D.
8. Thorlabs. <https://www.thorlabs.com/thorproduct.cfm?partnumber=WFS31-5C/M> Hartmann Shack on Thorlabs website.
9. Atchison, D. A., Scott, D. H. & Charman, W. N. Measuring ocular aberrations in the peripheral visual field using Hartmann-Shack aberrometry. *J. Opt. Soc. Am. A* **24**, 2963–2973. <https://opg.optica.org/josaa/abstract.cfm?URI=josaa-24-9-2963> (Sept. 2007).
10. Liang, J., Grimm, B., Goelz, S. & Bille, J. F. Objective measurement of wave aberrations of the human eye with the use of a Hartmann–Shack wave-front sensor. *J. Opt. Soc. Am. A* **11**, 1949–1957. <https://opg.optica.org/josaa/abstract.cfm?URI=josaa-11-7-1949> (July 1994).